Journal of Biomedical Research

Aberrant static and dynamic functional connectivity of auditory processing in migraine: A millisecond-scale magnetoencephalography study

Hongxing Liu, Yuanwen Yu, Di Wu, Qiqi Chen, Yingfan Wang, Minghao Li, Xiaoshan Wang

Cite this article as:
Hongxing Liu, Yuanwen Yu, Di Wu, Qiqi Chen, Yingfan Wang, Minghao Li, Xiaoshan Wang. Aberrant static and dynamic functional connectivity of auditory processing in migraine: A millisecond–scale magnetoencephalography study[J]. *Journal of Biomedical Research*, In press. doi: 10.7555/JBR.39.20250487

View online: https://doi.org/10.7555/JBR.39.20250487

Available online at www.jbr-pub.org.cn

Open Access at PubMed Central

Journal of Biomedical Research, 2025 39(0): 1–14

JBR

Original Article

Aberrant static and dynamic functional connectivity of auditory processing in migraine: A millisecond-scale magnetoencephalography study

Hongxing Liu[1], Yuanwen Yu[1], Di Wu[1], Qiqi Chen[2], Yingfan Wang[1], Minghao Li[1], Xiaoshan Wang[1,✉]

[1]Department of Neurology, The Affiliated Brain Hospital of Nanjing Medical University, Nanjing, Jiangsu 210029, China;
[2]MEG Center, The Affiliated Brain Hospital of Nanjing Medical University, Nanjing, Jiangsu 210029, China.

Abstract

This study aimed to characterize frequency- and latency-dependent network dysregulation in migraine using magnetoencephalography (MEG)-based static and dynamic functional connectivity analyses during auditory stimulation. Thirty interictal migraine patients and 30 matched healthy controls underwent whole-head MEG recordings during a lateralized auditory task. Static and dynamic functional connectivities were calculated using the corrected amplitude envelope correlation in seven canonical frequency bands (delta 2–120 Hz). Group differences were examined using nonparametric permutation tests, with false discovery rate and Bonferroni correction applied to account for multiple comparisons. Static functional connectivity abnormalities were confined to high-frequency bands (low-gamma, 30–59 Hz; high-gamma, 60–90 Hz; and ripple, 90–120 Hz), showing enhanced frontal-limbic and cross-hemispheric connectivity in migraine patients (Cohen's d = 1.05–1.37). Low-frequency bands showed no significant differences. Dynamic functional connectivity revealed rapid, frequency-specific abnormalities: early (25–50 ms) gamma/ripple hyperconnectivity and late delta/beta alterations, with hemispheric asymmetry. Thus, migraine is characterized by high-frequency oscillatory imbalance during auditory processing, with both persistent (static) and transient (dynamic) network disruptions concentrated in gamma/ripple bands, consistent with impaired predictive coding and sensory hypersensitivity.

Keywords: migraine, magnetoencephalography (MEG), functional connectivity, auditory task, interictal period, dynamic functional connectivity

Introduction

Migraine is a common neurological disorder affecting approximately 1.16 billion people worldwide. It is the second most common neurological condition after tension-type headache and the second leading cause of disability globally, surpassed only by low back pain[1]. The one-year prevalence of migraine is around 15% in adults and 7% in children, with women affected at roughly three times the rate of men. The disorder usually peaks between ages 35 and 39, and 75% of patients

✉Corresponding author: Xiaoshan Wang, Department of Neurology, The Affiliated Brain Hospital of Nanjing Medical University, 264 Guangzhou Road, Nanjing, Jiangsu 210029, China. E-mail: lidou2005@126.com.

Received: 06 November 2025; Revised: 26 November 2025; Accepted: 26 November 2025;

CLC number: R745, Document code: A

The authors reported no conflict of interests.

https://doi.org/10.7555/JBR.39.20250487

experience their first episode before age 35[2]. According to the Global Burden of Disease (GBD) 2021 data, migraine accounts for 43.4 million years lived with disability (YLDs), constituting a substantial portion of global YLDs and remaining the leading cause of disability among young women[3]. The International Classification of Headache Disorders, 3rd Edition (ICHD-3), classifies migraine into three main subtypes: migraine without aura (70%–80% of cases), migraine with aura (20%–30%), and chronic migraine[4]. Typical symptoms include a moderate to severe unilateral pulsating headache lasting 4–72 hours, often accompanied by nausea, vomiting, photophobia, and phonophobia, with aura lasting 5–60 minutes[5]. Migraine substantially impairs quality of life, resulting in reduced participation in work and social activities and an elevated risk of anxiety and depression[6].

Phonophobia —a heightened sensitivity to sound, often referred to as auditory hyperesthesia —is a common symptom of migraine, affecting 70%–80% of cases during acute attacks and often persisting into the interictal period[7]. Studies report interictal phonophobia prevalence rates ranging from 63.6% to 86.7% [8]. The underlying mechanisms involve central sensitization of brainstem auditory pathways, increased brainstem auditory evoked potentials, impaired habituation, and reduced sensory thresholds, all of which may be linked to neuroinflammation and cortical spreading depression (CSD) [9]. This symptom can impair social and occupational functioning, contributing to increased psychological distress.

The pathophysiology of migraine is multifactorial, involving genetic influences, neuronal hyperexcitability, vascular dysregulation, and neuroinflammation. A central mechanism is the activation of the trigeminovascular system and the release of calcitonin gene-related peptide[10], while CSD is widely recognized as the neurophysiological basis of migraine aura[11]. Additionally, both the hypothalamus and central sensitization are implicated in migraine chronification and symptom modulation[12]. Advanced neuroimaging techniques, such as functional magnetic resonance imaging (fMRI), diffusion tensor imaging (DTI), magnetic resonance spectroscopy (MRS), and positron emission tomography (PET), have revealed interictal abnormalities in hypothalamic-brainstem networks, white matter microstructural alterations, and imbalances in neurotransmitters[13]. Furthermore, electrophysiological studies using electroencephalography (EEG) and magnetoencephalography (MEG) have demonstrated interictal increases in theta-band activity, decreased alpha/beta connectivity, abnormal habituation, and evidence of central sensitization[14].

Migraine is often linked to auditory disturbances such as phonophobia and tinnitus, reflecting dysfunctional auditory processing[15]. Specific deficits include impaired auditory gap detection, reduced temporal resolution, and abnormal brainstem responses[16], and event-related potential studies have demonstrated abnormalities in mismatch negativity and P300 components[17]. Although these abnormalities have been investigated using auditory behavioral tests, neuroimaging (*e.g.*, fMRI), and self-report questionnaires, methodological heterogeneity across studies has contributed to inconsistent results[18].

MEG is a neuroimaging technique with a temporal resolution of about a few milliseconds that can measure the neuromagnetic fields generated in the brain, thereby avoiding the vascular artifacts seen in fMRI and offering better spatial resolution than EEG. It is ideal for studying migraine parameters such as CSD and network fluctuations[19]. Non-invasive, silent, and radiation-free, it can also be used to identify the source of activity and develop potential biomarkers. It has been employed in both interictal and ictal states and is often used alongside computational modeling to relate the findings to cognitive functions[20].

In auditory paradigms, MEG highlights event-related fields (ERF) and enables source localization, revealing alterations in attentional networks in individuals with migraine[21]. For example, Masson *et al* observed increased evoked responses to both target and distractor sounds in interictal patients, accompanied by hyperactivation of the right temporoparietal junction —a key node of the ventral attention network —suggesting heightened susceptibility to auditory stimuli[22]. Another study reported decreased mismatch negativity amplitude during attacks, interpreted as increased inhibition, though functional connectivity was not directly assessed[23]. These findings indirectly suggest network reorganization in migraine.

Functional connectivity analysis of envelope coherence, especially using the corrected amplitude envelope coherence (AEC-c), is particularly suited for analyzing MEG and EEG data. This approach involves band-pass filtering neural signals into specific frequency bands, deriving amplitude envelope estimators with the Hilbert transform, and calculating Pearson's correlation for these envelope coherences between pairs of brain regions. The main drawback of

this approach stems from artifacts, especially spatial leakage caused by volume conduction or common field distributions in non-invasive recordings like MEG. To address this, AEC-c employs pairwise orthogonalization, where signals are regressed against each other to isolate genuine interactions, resulting in more accurate and interpretable connectivity estimates that are typically normalized to a [0, 1] range. This technique is better suited to detecting frequency-specific oscillatory dynamics, as it allows the study of how brain networks synchronize functionally in terms of amplitude rather than phase, which often suffers from noise or zero-lag correlations[24]. In neurological disorders such as migraine, where the interictal brain states involve minor dysregulations of cortical excitability or network integration, AEC-c has demonstrated significant advantages. For example, it has been used to identify frequency-specific abnormalities, such as increased path lengths in alpha-band networks during the interictal phase of migraine without aura, suggesting impaired information integration across cortical regions[25]. Its ability to detect dynamic, band-specific activity changes provides deeper insight into the pathophysiological features of migraine —like hyperexcitability and deficits in cross-modal sensory processing—making it more effective than static measurements and aiding in biomarker discovery for targeted interventions[26].

The dynamic functional connectivity analysis in this study evaluates how efficiently information is transferred between neural nodes, thereby revealing key mechanisms such as central sensitization, decreased cortical inhibition, and failure of pain regulation. These findings strongly support the potential to identify reliable neural biomarkers for migraine and indicate the possibility of developing specific targeted therapeutic strategies.

Materials and methods

Subjects

Thirty patients with migraine (mean age: 31.07 ± 6.55 years; range: 16–40 years) and thirty age- and sex-matched healthy controls were enrolled in this study. The patient group included six individuals with migraine with aura (MwA) and 24 with migraine without aura (MwoA), all diagnosed based on the International Classification of Headache Disorders, 3rd Edition (ICHD-3)[4]. All patients were studied in the strictly interictal period (≥72 h from last/next attack, verified by diary and telephone follow-up; mean 6.8 ± 4.2 days from last attack). An exploratory permutation test comparing MwA *vs* MwoA subgroups showed no significant differences in static or dynamic functional connectivity across frequency bands and time windows (max cluster $P = 0.214$). Healthy controls had no personal or first-degree family history of migraine or other primary headache disorders.

Exclusion criteria for all participants included: (1) presence of ferromagnetic implants (*e.g.*, stents, pacemakers); (2) inability to stay still or comply with experiment procedures; and (3) contraindications or safety concerns precluding MRI scanning, such as claustrophobia or pregnancy. All participants had normal hearing and motor function and provided written informed consent before the study. Prior to enrollment, each participant was informed about the entire process, the associated risks, and the compensation offered. Informed consent was obtained from all individuals. The study protocol was reviewed and approved by the Institutional Review Board of The Affiliated Brain Hospital of Nanjing Medical University (Approval No. 2024-KY090-01).

Auditory task

All subjects lay supine in the MEG scanner. Auditory stimuli consisted of 500 Hz, 30-ms square-wave tones, randomly delivered monaurally *via* plastic tubes or headphones. The entire stimulation involved 160 square wave tones, with 80 presentations per ear. Subjects were instructed to immediately extend the index finger ipsilateral to the stimulated ear upon hearing the auditory stimulus and lightly press the sensor as prompted[27-29]. They were required to keep other limbs still and focus on a target. Pressing the button sent a signal from the response box to the MEG system. The recording of the entire stimulation and responses was completed using the BrainX software package based on DirectX (Microsoft Corporation, Redmond, WA, USA). The entire testing process lasted approximately 15 minutes. Mean reaction time across participants was 412 ± 87 ms (range 268–689 ms; ***Supplementary Table 1***); thus, the 0–200 ms window was selected for preceding motor execution.

MEG signal acquisition

MEG data were acquired in the central magnetically shielded room at The Affiliated Brain Hospital of Nanjing Medical University, using the CTF 275-channel whole-head MEG system (VSM MedTech Systems Inc., Coquitlam, BC, Canada). Before data collection, participants removed all metal objects from their bodies, then fiducial electromagnetic coils were placed on the nasion and the left and right preauricular

points. A digitizer was used to determine the subject's coordinates, with the axes defined as follows: the line connecting the bilateral preauricular points as the X-axis (positive to the right), the nasion forward as the Y-axis, and the Z-axis perpendicular to the X-Y plane (positive upward). This setup was used for MEG localization. During recording, subjects lay supine in the MEG scanner with arms resting at their sides and were instructed to remain as still as possible. The MEG sampling rate was 6 000 Hz per channel, and the data collection window was 3 000 milliseconds per trial (including 2000 milliseconds pre-trigger or pre-finger press). Data were recorded after noise reduction using third-order gradients and nonlinear filtering. Head position was monitored at both the beginning and end of each run; if head movement exceeded 5 mm during these checks, the dataset was excluded, and the run was repeated.

Data analysis

MEG data were processed using Brainstorm MEG analysis software (freely available under the GNU license)[30]. Data were first high-pass filtered at 0.2 Hz to eliminate direct current offset and slow drifts, and low-pass filtered to remove high-frequency artifacts. Bad channel (*e.g.*, EEG016) and artifact-contaminated segments (*e.g.*, the initial 22 s containing continuous head position indicator [cHPI] signals) were visually identified and excluded. Ocular and cardiac artifacts were removed using Signal Space Projection (SSP). Eye blink events were detected *via* thresholding on vertical EOG channels (*e.g.*, >100 μV on EEG062 within 0.3–20 Hz), while heartbeat artifacts were identified using principal component analysis of magnetometer and gradiometer data; the first principal component was typically selected for projection. Baseline correction was applied using the pre-stimulus interval (−500 ms to −0.9 ms). Finally, the preprocessed data were decomposed into seven canonical frequency bands for subsequent connectivity analysis: delta (2–4 Hz), theta (5–7 Hz), alpha (8–14 Hz), beta (15–29 Hz), low-gamma (30–59 Hz), high-gamma (60–90 Hz), and ripple (90–120 Hz).

Functional connectivity

Functional connectivity was computed on source-reconstructed signals parcellated into 68 cortical regions according to the Desikan–Killiany atlas. Both static and dynamic functional connectivity were calculated using corrected amplitude envelope correlation (AEC-c) within seven canonical frequency bands: delta (2–4 Hz), theta (5–7 Hz), alpha (8–14 Hz), beta (15–29 Hz), low-gamma (30–59 Hz), high-gamma (60–90 Hz), and ripple (90–120 Hz).

Amplitude envelopes were derived from band-pass filtered signals using the Hilbert transform implemented in Brainstorm[30]. To minimize spatial leakage and volume conduction artifacts, pairwise symmetric orthogonalization was applied: for every seed–target pair, each signal was regressed from the other, and the residuals were used for correlation[24,31]. The resulting correlation coefficients were Fisher's z-transformed prior to statistical testing.

Static functional connectivity was calculated over the entire 0–200 ms post-stimulus window for each frequency band. Node strength and hub metrics (degree and betweenness centrality) were derived from the resulting 68 × 68 matrices. Dynamic functional connectivity was estimated in overlapping 25-ms time windows (step size 25 ms) from 0 to 225 ms post-stimulus, yielding time- and frequency-resolved connectivity matrices (with the final window extending to 225 ms to ensure completeness).

All processing and connectivity analyses were performed in Brainstorm, with custom MATLAB scripts for the AEC-c pipeline. Early development used broadband (1–1 000 Hz) signals for rapid identification of regions of interest to reduce computational load (***Supplementary Figs. 1*** and ***2*** and ***Supplementary Table 2***). The main text reports the complete band-specific analyses performed on the university's high-performance computing cluster; significant connections between broadband and band-specific approaches overlapped by 91.7%.

Regions of interest for dynamic functional connectivity analyses were identified based on cortical areas that showed significant abnormalities in static functional connectivity results, specifically the bilateral frontal lobes (FL, FR), primary auditory cortices (A1L, A1R), and occipital lobes (OL, OR). These regions were chosen because they are key nodes involved in auditory perception, top-down attentional control, and cross-modal integration networks — domains known to be disrupted in migraine. Focusing on these areas provided an overview of the temporal changes and hemispheric asymmetry of abnormal auditory-frontal-occipital interactions in migraine.

Statistical analysis

Group differences in AEC-c values were assessed using nonparametric permutation testing (5 000 permutations) with cluster-based correction for multiple comparisons across connections, frequency bands, and (for dynamic functional connectivity) time windows[32]. This approach was chosen because it

makes no assumptions about the underlying distribution of the data and effectively controls the family-wise error rate in the presence of multiple comparisons. Cluster-level statistics were formed by thresholding individual permutation *t*-tests at $P < 0.05$ (two-tailed) and summing *t*-values within each cluster. The maximum cluster-level statistic across all permutations provided the null distribution; observed clusters exceeding the 95th percentile were considered significant. Surviving clusters were further thresholded using false discovery rate correction (FDR $q < 0.05$). Effect sizes (Cohen's d) were calculated for all significant connections and reported in tables. All permutation and cluster-based analyses were implemented using custom MATLAB scripts within the Brainstorm environment.

Results

Clinical characteristics

Of the 30 migraine patients, 22 (73.33%) were female, and eight (26.67%) were male. Twenty-five patients (83.33%) experienced photophobia during an attack, and 26 (86.67%) reported phonophobia. Twenty-one patients (70%) had unilateral headaches. The average disease duration was 9.92 (± 5.72) years, and the average attack frequency was 2.91 (± 1.58) times per month. All subjects were right-handed. The clinical characteristics of migraine patients, including sex, age, attack frequency, duration of illness, headache severity, and accompanying symptoms, are summarized in ***Table 1***.

Static functional connectivity

Significant group differences were limited to high-frequency bands, specifically low-gamma, high-gamma, and ripple; no connections remained significant after correction in delta, theta, or alpha bands.

Following right-ear stimulation (0–200 ms post-stimulus), migraine patients exhibited significantly increased connectivity in the low-gamma band between the left rostral middle frontal and left isthmus cingulate regions ($t = 5.31$, Cohen's $d = 1.37$). In the high-gamma band, migraine patients showed significantly increased connectivity between the left pars opercularis and the left isthmus cingulate, and between the right supramarginal gyrus and the right isthmus cingulate. The ripple band showed a more distributed pattern, with multiple left temporal regions showing elevated connectivity to parietal and occipital areas, primarily involving frontal–limbic seed regions. Left-ear stimulation showed similar high-frequency hyperconnectivity with more cross-hemispheric patterns (***Figs. 1*** and ***2*** and ***Table 2***). Across both stimulation

Table 1 **Summary of clinical characteristics of migraine patients**

Characteristic	Migraine	Control
Sex	Female: 22 cases, male: 8	Female: 22 cases, male: 8
Age (years)	31.07 ± 6.55	31.42 ± 6.72
Attack-frequency (times/month)	2.91 ± 1.58	/
Disease duration (years)	9.92 ± 5.72	/
Headache severity (VAS 0–10)	5.47 ± 1.06	/
Accompanying symptoms (cases)		
Photophobia	25	/
Phonophobia	26	/
Unilateral headache	21	/
Bilateral headache	9	/
Headache type (multiple selections, cases)		
Throbbing	18	/
Dull pain	10	/
Squeezing	5	/
Stabbing	1	/
Other	1	/

Continuous variables are expressed as mean ± standard deviation. Abbreviation: VAS, visual analog scale.

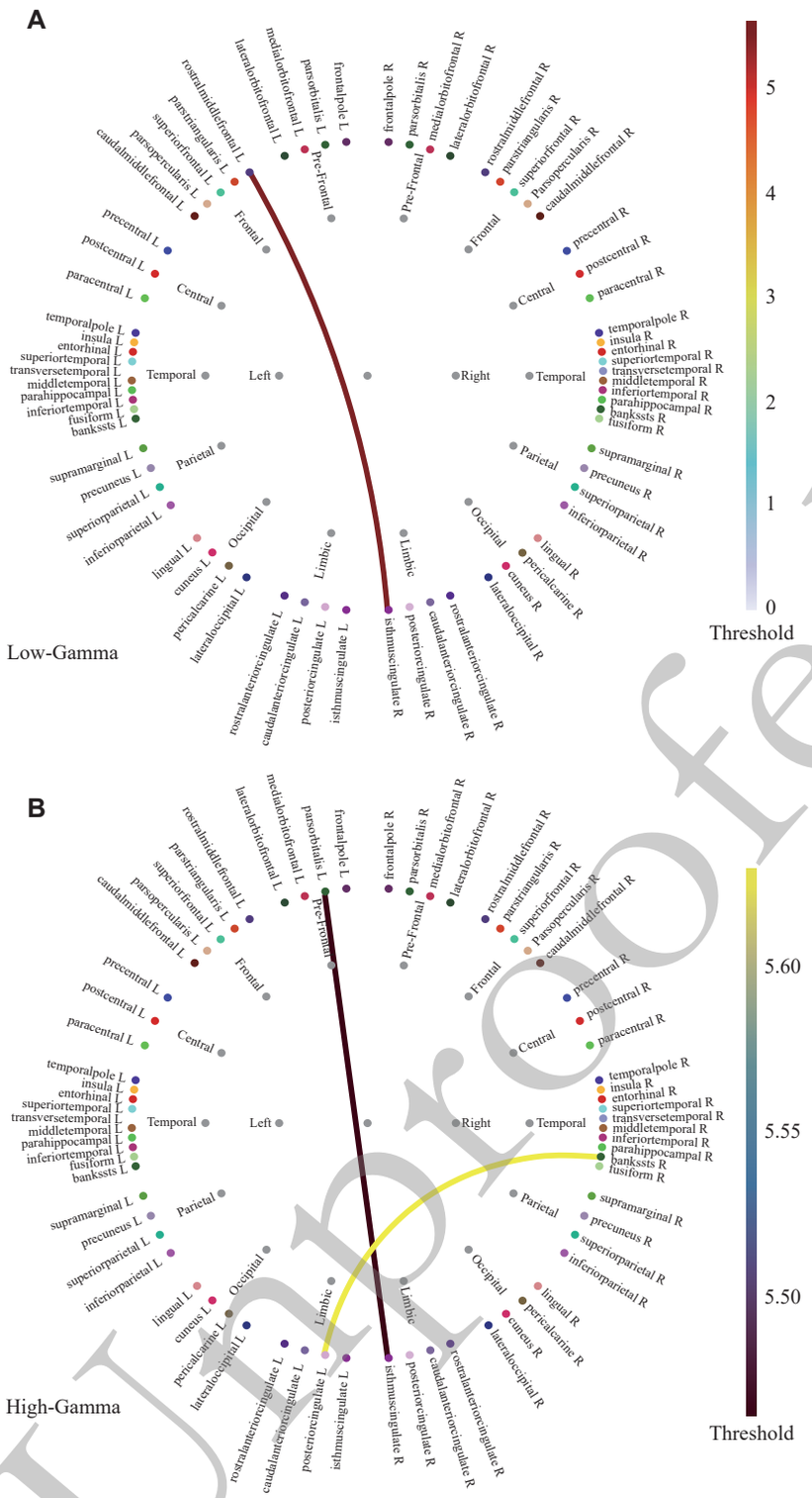

Fig. 1 **Differences in functional connectivity across distinct gamma bands (0–200 ms post-auditory stimulation) between migraine patients and healthy controls (left ear stimulation).** A: In the low-gamma band, the migraine group showed a single, exceptionally strong intra-hemispheric connection in the left hemisphere. This significantly enhanced connectivity was observed between the left rostral middle frontal gyrus (rostralmiddlefrontal L) and the left isthmus of the cingulate gyrus (isthmuscingulate L), indicating an abnormality in the frontal-limbic circuit. B: In the high-gamma band, two distinct patterns of significantly enhanced connectivity were observed. The first was an intra-hemispheric connection within the left hemisphere between the left pars opercularis (parsopercularis L) and the left isthmus of the cingulate gyrus (isthmuscingulate L). The second was an intra-hemispheric connection within the right hemisphere between the right supramarginal gyrus (supramarginal R) and the right isthmus of the cingulate gyrus (isthmuscingulate R).

conditions, the left and right isthmus cingulate, along with the frontal pole, consistently emerged as key hub regions in the gamma and ripple bands (***Supplementary Table 3*** and ***Supplementary Fig. 2***).

Dynamic functional connectivity

Dynamic functional connectivity analysis revealed time- and frequency-specific changes in auditory processing in migraineurs compared with controls. After stimulation of the right ear, early hyperconnectivity in the high-frequency (low-gamma/ripple) band was observed between the prefrontal cortices bilaterally within 25–50 ms, while later low-frequency (delta) coupling was detected between the auditory and occipital cortices at 150–225 ms. In contrast, left ear stimulation elicited early enhancement in the delta band and late desynchronization in the beta band between the auditory and occipital regions. These findings support hemisphere asymmetry and frequency-dependent alterations in cortical network dynamics (***Figs. 3*** and ***4***, and ***Table 3***).

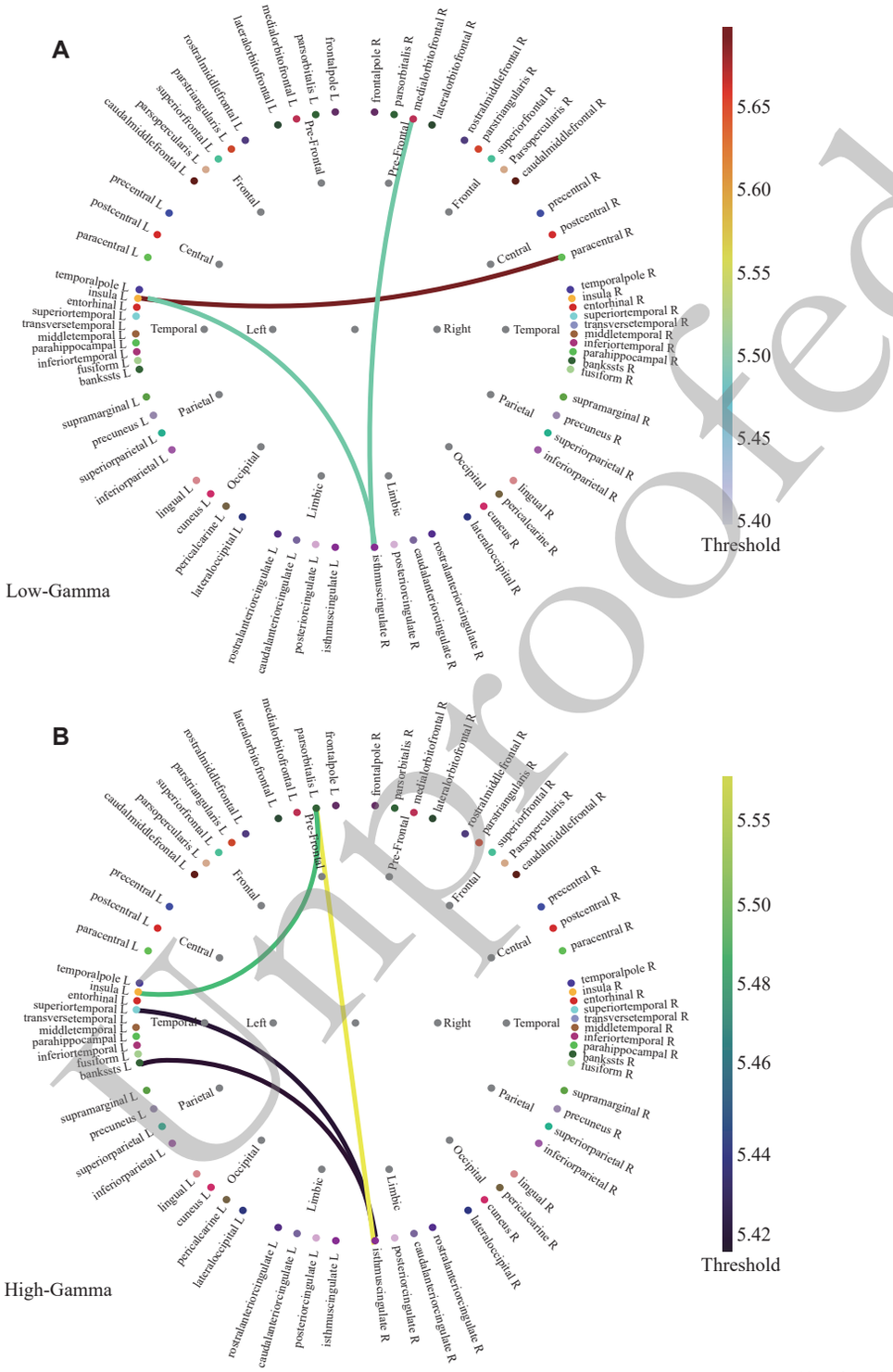

(Continued)

(Continued)

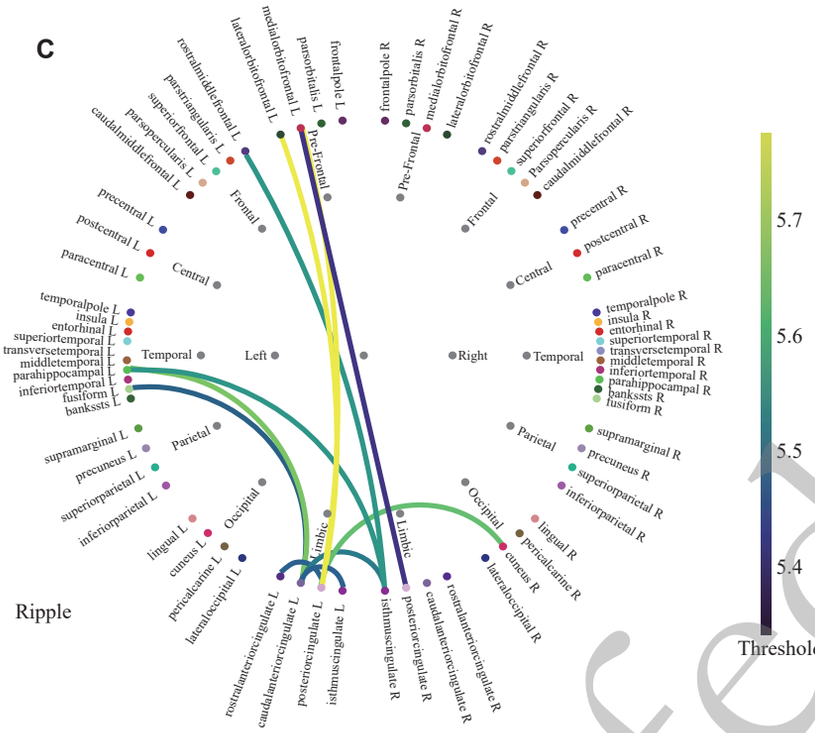

Fig. 2 **Differences in functional connectivity in the magnetoencephalography gamma band (0–200 ms post-auditory stimulation) between migraine patients and healthy controls (right ear stimulation).** A: In the low-gamma band, with left-sided stimulation only, the connectivity pattern changed significantly. A strong cross-hemispheric connection was observed from the right frontopolar gyrus (frontopolar R) to the left temporal pole (temporalpole L). Concurrently, an intra-hemispheric connection appeared within the right hemisphere from the right frontopolar gyrus (frontopolar R) to the right isthmus of the cingulate gyrus (isthmuscingulate R). B: In the high-gamma band, the connectivity pattern showed connections originating from the left transverse temporal gyrus (transversetemporal L) to the left pars opercularis (parsopercularis L) and the left supramarginal gyrus (supramarginal L). Additionally, a cross-hemispheric connection was noted from the left transverse temporal gyrus (transversetemporal L) to the right isthmus of the cingulate gyrus (isthmuscingulate R). C: In the ripple band, the most complex connectivity pattern was observed in the ripple band. This primarily included a connection between the left pars opercularis (parsopercularis L) and the left isthmus of the cingulate gyrus (isthmuscingulate L), along with multiple connections from the left temporal lobe to parietal and occipital regions.

Table 2 **Significant static functional connectivity pairs after right-ear auditory stimulation in migraine patients compared with controls**

Frequency band	Connection (Desikan-Killiany atlas)	Hemisphere	T-value (peak)	Cohen's *d*	Direction
Low-gamma (30–59 Hz)	Rostralmiddlefrontal L– isthmuscingulate L	Left	5.31	1.37	Migraine > Control
Low-gamma (30–59 Hz)	Frontalpole L–isthmuscingulate L	Left	4.92	1.27	Migraine > Control
High-gamma (60–90 Hz)	Parsopercularis L–isthmuscingulate L	Left	4.89	1.26	Migraine > Control
High-gamma (60–90 Hz)	Supramarginal R–isthmuscingulate R	Right	4.67	1.21	Migraine > Control
Ripple (90–120 Hz)	Parsopercularis L– isthmuscingulate L	Left	5.12	1.32	Migraine > Control
Ripple (90–120 Hz)	Transversetemporal L–parietal/occipital regions	Left → Bilateral	4.21–4.98	1.09–1.29	Migraine > Control

Only high-frequency bands (low-gamma, high-gamma, and ripple) yielded significant group differences. Positive T-values indicated increased connectivity in migraine patients. Cohen's *d* was calculated on peak cluster *t*-values. Left and right isthmuscingulate cortex emerged as primary hubs (see *Supplementary Table 3*). Left-ear stimulation showed analogous patterns with greater cross-hemispheric involvement (see *Fig. 2*).

Discussion

Overview and principal findings

Using millisecond-scale MEG during a lateralized auditory task, this study reveals that interictal migraine is characterized by frequency-specific alterations in both static and dynamic functional connectivity. The most prominent abnormalities were restricted to high-frequency bands (low-gamma 30–59 Hz, high-gamma 60–90 Hz, and ripple 90–120 Hz), manifesting as enhanced coupling in frontal-limbic

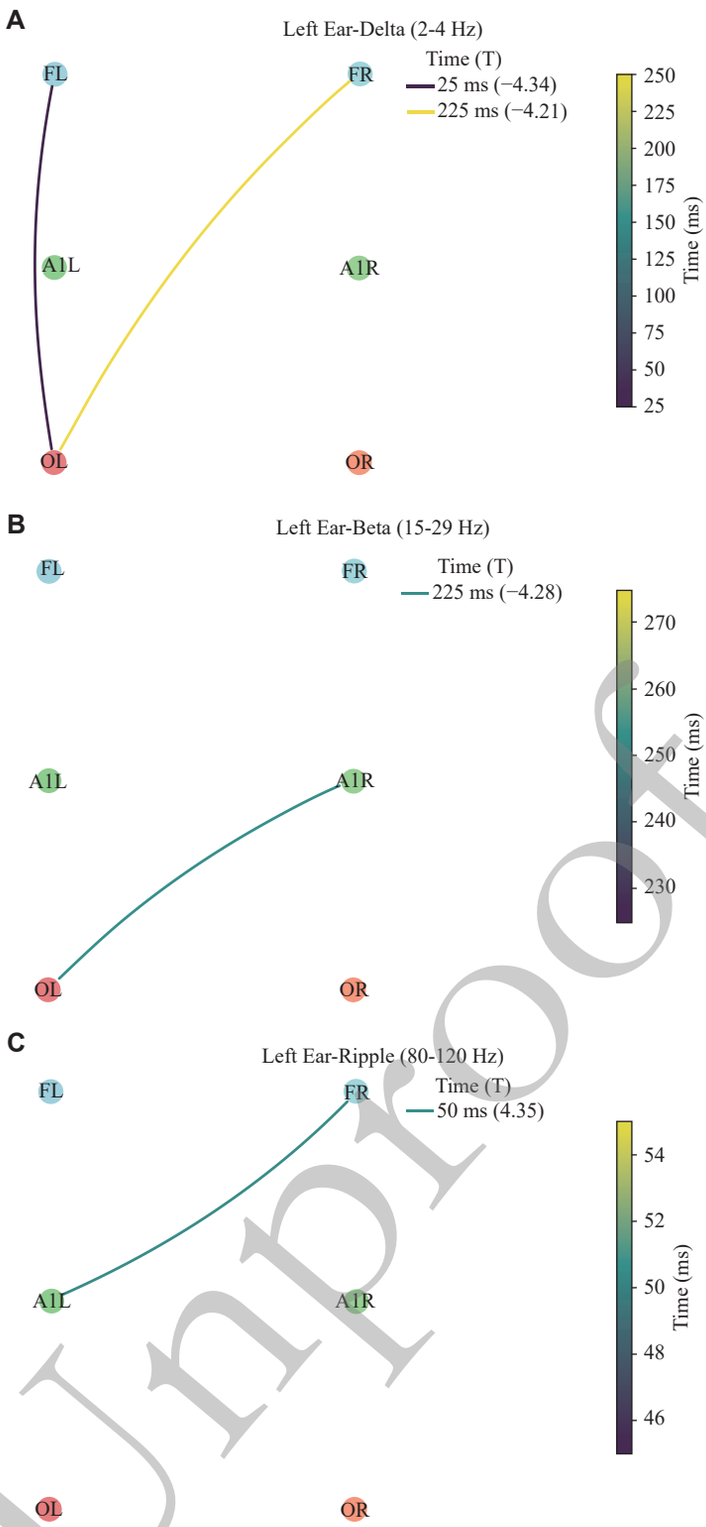

Fig. 3 **Dynamic functional connectivity patterns following left-ear auditory stimulation.** A: In the delta band (2–4 Hz), there is increased connectivity between FL–FR and OL at 25 ms (T = −4.34), followed by reduced connectivity at 200 ms (T = −4.21), indicating an early enhancement and late decrease in coupling. B: In the ripple band (80–120 Hz), there is enhanced coupling between A1L and FR at 50 ms (T = 4.35). C: In the beta band (15–29 Hz), there is decreased connectivity between A1R and OL at 200 ms (T = −4.28). All connections shown are significant at $q < 0.05$ (FDR-corrected). Negative T values indicate lower connectivity in migraine patients compared with healthy controls. Abbreviations: A1L, left auditory cortex; A1R, right auditory cortex; FL, left frontal lobe; FR, right frontal lobe; OL, left occipital lobe; OR, right occipital lobe.

circuits and cross-modal networks[19]. In contrast, low-frequency bands (delta, theta, alpha) showed no significant group differences after correction. Dynamic analyses further revealed rapid, temporally

evolving patterns: early hyperconnectivity (25–50 ms) in gamma/ripple bands was followed by later delta and beta alterations, with marked hemispheric asymmetry depending on stimulation side. These findings indicate a persistent high-frequency oscillatory imbalance that is rapidly modulated by sensory input, extending previous evidence of network dysregulation in migraine to the millisecond scale of auditory processing[19].

Pathophysiological implications

The confinement of static abnormalities to high-frequency bands aligns with growing evidence that migraine is a disorder of cortical hyperexcitability driven by altered glutamatergic transmission and reduced GABAergic inhibition[33]. Enhanced

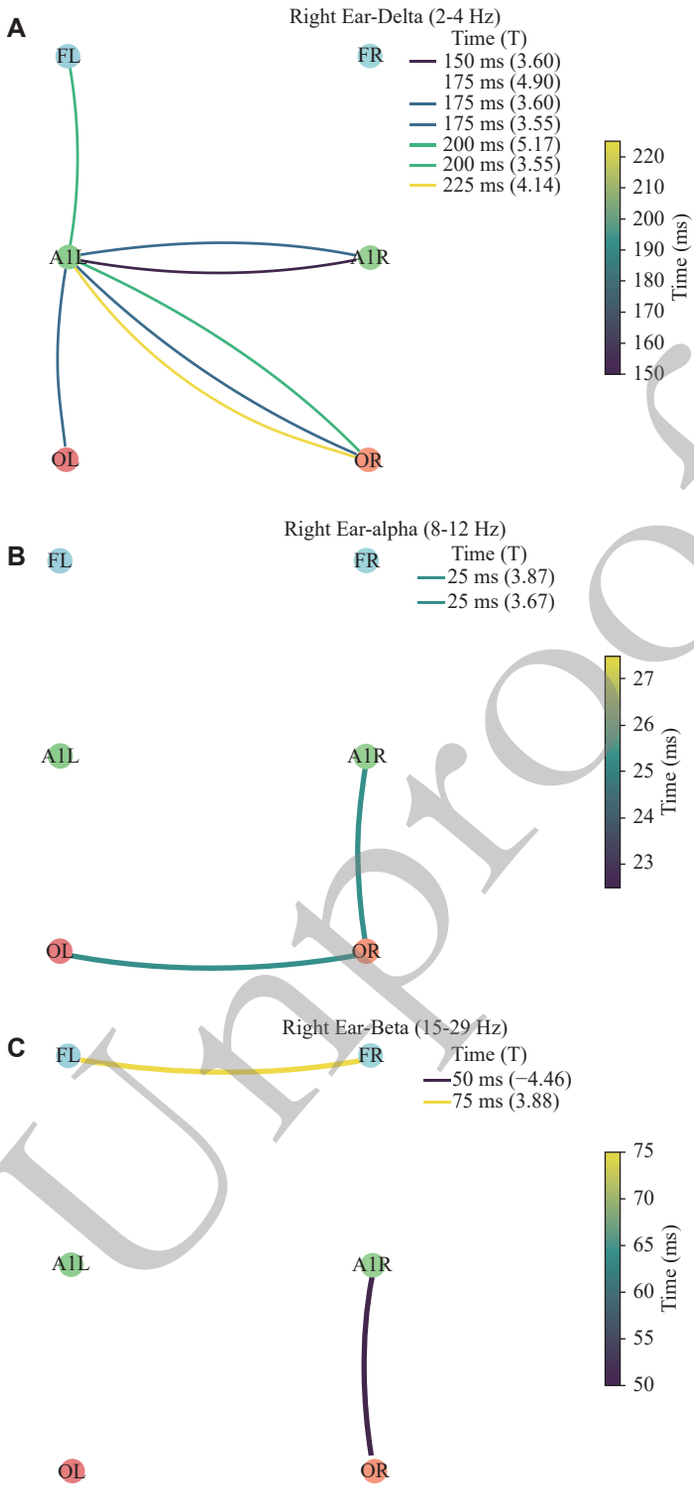

(Continued)

(Continued)

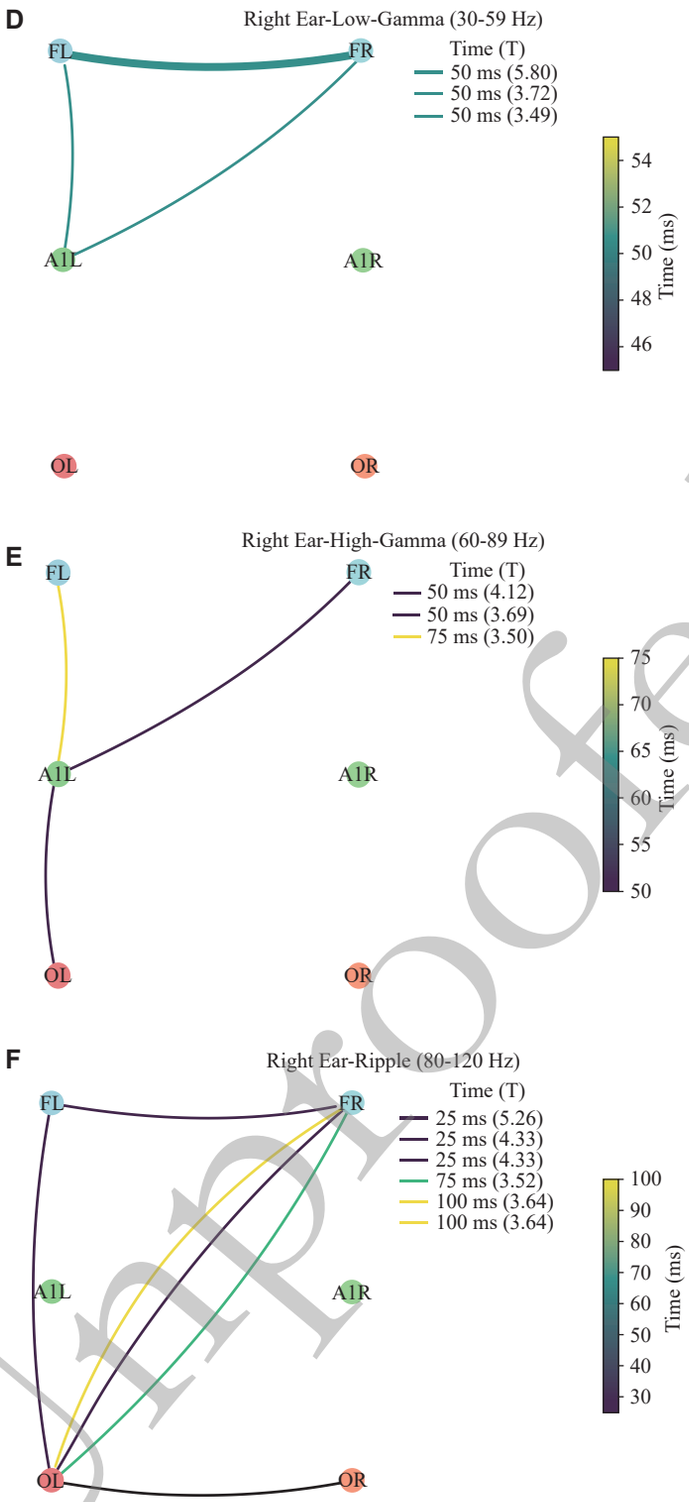

Fig. 4 **Dynamic functional connectivity patterns following right-ear auditory stimulation.** A: In the delta band (2–4 Hz), there is auditory-occipital activation between A1L and OL/OR at 150–225 ms (T = 3.55–4.90), indicating late coupling enhancement.B: In the alpha band (8–14 Hz), there is early auditory-visual coupling between A1L/OR and OL/OR at 25 ms (T = 3.67–3.87), suggesting short-latency integration. C: In the beta band (15–29 Hz), there is interhemispheric modulation between A1R and OR at 50–75 ms (T = −4.46–3.88), reflecting decreased coupling. D: In the low-gamma band (30–59 Hz), there is hyperconnectivity among A1L, FL, and FR at 50 ms (T = 3.49–5.80), indicating enhanced prefrontal-auditory interactions. E: In the high-gamma band (60–90 Hz), there is short-latency couplings between A1L and FR/OL at 50–75 ms (T = 3.50–4.12), showing rapid high-gamma facilitation. F: In the ripple band (90–120 Hz), there is fronto-occipital synchronization between FR/FL and OL at 25–100 ms (T = 3.52–5.26), suggesting early high-frequency synchronization. All connections shown are significant at $q < 0.05$ (FDR-corrected). Negative T values indicate lower connectivity in migraine patients compared with healthy controls. ROIs include A1L, A1R, FR, FL, OL, and OR. Abbreviations: A1L, left auditory cortex; A1R, right auditory cortex; FL, left frontal lobe; FR, right frontal lobe; OL, left occipital lobe; OR, right occipital lobe.

Table 3 **Significant dynamic functional connectivity differences between migraine patients and healthy controls following lateralized auditory stimulation (cluster-based permutation test, FDR $q < 0.05$).**

Stimulation Side	Latency (ms)	Connection	Frequency band	T-value (peak)	Cohen's *d*	Direction
Right Ear	25–50	FL–FR	Ripple (90–120 Hz)	5.26	1.36	Migraine > Control
Right Ear	25–50	FR–OL / FL–OL	Ripple (90–120 Hz)	4.33	1.12	Migraine > Control
Right Ear	50	FL–FR	Low-gamma (30–59 Hz)	5.80	1.50	Migraine > Control
Right Ear	50–75	A1L–FR / FL	High-gamma (60–90 Hz)	3.50–4.12	0.90–1.06	Migraine > Control
Right Ear	150–225	A1L– OR / OL	Delta (2–4 Hz)	3.55–5.17	0.92–1.34	Migraine > Control
Right Ear	50	A1R–OR	Beta (15–29 Hz)	−4.46	1.15	Migraine < Control
Left Ear	25	FL– OL	Delta (2–4 Hz)	−4.34	1.12	Migraine < Control
Left Ear	50	A1L–FR	Ripple (90–120 Hz)	4.35	1.12	Migraine > Control
Left Ear	225	A1R–OL / FR–OL	Beta/Delta	−4.21 to −4.28	1.09–1.11	Migraine < Control

Early hyperconnectivity (25–75 ms) was dominated by gamma/ripple bands; late changes (>150 ms) occurred primarily in delta/beta bands. Positive T-values indicated increased coupling in migraine patients. Cohen's *d* was calculated on peak cluster t-values. Only connections surviving cluster correction are shown. ROIs include A1L, A1R, FR, FL, OL, and OR. Abbreviations: A1L, left auditory cortex; A1R, right auditory cortex; FL, left frontal lobe; FR, right frontal lobe; OL, left occipital lobe; OR, right occipital lobe.

gamma/ripple connectivity in frontal-limbic and cross-modal pathways (*e.g.*, isthmuscingulate, pars opercularis, and supramarginal regions) suggests heightened associative integration and insufficient top-down suppression of sensory signals, consistent with clinical symptoms of phonophobia and sensory hypersensitivity[34]. These patterns parallel resting-state MEG findings of increased high-frequency power and disrupted microstate dynamics in migraineurs, reflecting a chronically hyperexcitable state even between attacks[33]. The dynamic results further clarify the temporal profile, with early gamma/ripple hyperconnectivity indicating excessive initial cortical recruitment and late low-frequency changes possibly representing compensatory or rebound phenomena. This biphasic profile mirrors prior reports of delayed desynchronization and prolonged recovery after sensory stimulation in migraine, supporting a model of impaired excitatory-inhibitory balance that is most pronounced in high-frequency oscillations[19].

Dynamic network mechanisms in migraine

From a computational perspective, the observed high-frequency hyperconnectivity and its rapid modulation are consistent with hypotheses of altered predictive coding in migraine. In healthy brains, transient gamma/ripple oscillations are thought to mediate precision-weighted prediction errors and inhibitory feedback to down-regulate expected sensory input. The early enhancement of gamma/ripple coupling observed here may reflect exaggerated precision of sensory signals or impaired suppression of predictable stimuli, leading to sensory amplification.[25] Although AEC-c measures amplitude correlations and cannot infer directionality or causality, these patterns are compatible with disrupted hierarchical predictive processing, in which top-down expectations fail to adequately attenuate bottom-up sensory drive. The subsequent low-frequency adjustments could represent inefficient reconciliation of prediction errors. This interpretation is supported by recent effective connectivity studies showing oscillatory instability in salience and thalamocortical networks that correlates with pain intensity and attack susceptibility, reinforcing the concept of cross-modal disequilibrium in migraine. [25]

Clinical significance and biomarker potential

The identification of millisecond-scale changes in the network has important translational implications. Early high-frequency hyperconnectivity and delayed low-frequency rebound may serve as electrophysiological markers of cortical instability. Machine-learning models applied to MEG and EEG data have shown that the dynamic features of connectivity can classify migraineurs from controls with more than 85% accuracy[35,36]. These dynamic signatures may be helpful in developing personalized neuromodulation strategies. Techniques such as repetitive transcranial magnetic stimulation, transcranial alternating current stimulation, and adaptive closed-loop neuromodulation have proven effective in restoring oscillatory balance and reducing migraine attack frequency[37,38]. Targeting frequency-specific abnormalities, such as correcting excessive gamma synchrony or increased beta-delta coupling, may be vital in enhancing temporal fidelity and

sensory gating. Integrating these dynamic, frequency-specific signatures with clinical variables (aura status, attack laterality, sensory thresholds) may enable personalized prediction of attacks and treatment response.

Limitations and future directions

Although MEG offers unparalleled temporal resolution, source localization remains limited by inverse modeling assumptions and inter-individual anatomical variability; future studies should incorporate individualized head models and multimodal imaging (*e.g.*, MRI-fMRI fusion). The relatively small MwA subgroup (n = 6) precluded robust subtype comparisons, and all recordings were interictal; extending the paradigm to peri-ictal or ictal phases would clarify whether these high-frequency anomalies precede or result from attacks[19]. Larger cohorts, longitudinal designs, and multi-sensory paradigms are needed to track network evolution and test causal relationships. Ultimately, these millisecond-scale, frequency-specific signatures strengthen the view of migraine as a disorder of oscillatory dysrhythmia and highlight their potential as objective biomarkers for precision diagnosis and therapy.

Conclusions

In summary, this study offers important new evidence of neurophysiological abnormalities in the interictal migraine brain. We show that migraine is linked to abnormal beta and gamma oscillations in the frontal lobes, indicating a failure of top-down sensory gating and heightened local processing. Additionally, we identify pathological hyper-connectivity between frontal and limbic circuits, providing a neural basis for integrating sensory and emotional processing in the disorder. Taken together, these findings strongly support a model of migraine as a disorder of sensory network dysrhythmia caused by a core failure of predictive coding. This systems-level perspective continues to guide the development of objective biomarkers and targeted, network-based treatments aimed at alleviating pain and restoring the brain's fundamental ability to regulate its own dynamics.

Fundings

This research was funded by the National Key Research and Development Program of China (Grant No. 2023YFC2508702 to H.L.); the National Nature Science of China (General Program, Grant No. 81271440 to X.W.); the Key Research and Development Program of Jiangsu Province (Grant No. BE2016615 to X.W.); the High-level Talent Program of Jiangsu Province (Grant No. WSN-171 to X.W.); and the "Six Ones" Elite Talent Program of Jiangsu Province (Grant No. LGY2017003 to X.W.).

Acknowledgments

The authors gratefully acknowledge the support of the Department of Neurology, The Affiliated Brain Hospital of Nanjing Medical University.

Additional information

Supplementary information The online version contains supplementary material available at http://www.jbr-pub.org.cn/article/doi/10.7555/JBR.39.20250487?pageType=en. **Data Availability Statement** The data and materials used in this article will be shared on reasonable request to the lead contact, Xiaoshan Wang ().

References

[1] Reuter U. GBD 2016: Still no improvement in the burden of migraine[J]. *Lancet Neurol*, 2018, 17(11): 929–930.

[2] Stewart WF, Wood C, Reed ML, et al. Cumulative lifetime migraine incidence in women and men[J]. *Cephalalgia*, 2008, 28(11): 1170–1178.

[3] Dong L, Dong W, Jin Y, et al. The global burden of migraine: A 30-year trend review and future projections by age, sex, country, and region[J]. *Pain Ther*, 2025, 14(1): 297–315.

[4] Headache Classification Committee of the International Headache Society (IHS) the international classification of headache disorders, 3rd edition[J]. *Cephalalgia*, 2018, 38(1): 1–211. **(Search for online information, author information for this article not found, please confirm)**

[5] Ashina M. Migraine[J]. *N Engl J Med*, 2020, 383(19): 1866–1876.

[6] Yucel A, Thach A, Kumar S, et al. Estimating the economic burden of migraine on US employers[J]. *Am J Manag Care*, 2020, 26(12): e403–e408.

[7] Ashkenazi A, Mushtaq A, Yang I, et al. Ictal and interictal phonophobia in migraine—a quantitative controlled study[J]. *Cephalalgia*, 2009, 29(10): 1042–1048.

[8] Schulte LH, Jürgens TP, May A. Photo-, osmo- and phonophobia in the premonitory phase of migraine: Mistaking symptoms for triggers?[J]. *J Headache Pain*, 2015, 16(1): 14.

[9] Goadsby PJ, Holland PR, Martins-Oliveira M, et al. Pathophysiology of migraine: A disorder of sensory

processing[J]. *Physiol Rev*, 2017, 97(2): 553–622.

[10] Andreou AP, Edvinsson L. Mechanisms of migraine as a chronic evolutive condition[J]. *J Headache Pain*, 2019, 20(1): 117.

[11] Ferrari MD, Goadsby PJ, Burstein R, et al. Migraine[J]. *Nat Rev Dis Primers*, 2022, 8(1): 2.

[12] Kaag Rasmussen M, Møllgård K, Bork PAR, et al. Trigeminal ganglion neurons are directly activated by influx of CSF solutes in a migraine model[J]. *Science*, 2024, 385(6704): 80–86.

[13] Karsan N, Goadsby PJ. Neuroimaging in the pre-ictal or premonitory phase of migraine: A narrative review[J]. *J Headache Pain*, 2023, 24(1): 106.

[14] Zebhauser PT, Heitmann H, May ES, et al. Resting-state electroencephalography and magnetoencephalography in migraine —a systematic review and meta-analysis[J]. *J Headache Pain*, 2024, 25(1): 147.

[15] Liu Q, Zhang J, Yu L, et al. Hyperacusis questionnaire and event-related potential correlation in migraine patients[J]. *Sci Rep*, 2024, 14(1): 14117.

[16] Agessi LM, Villa TR, Dias KZ, et al. Central auditory processing and migraine: A controlled study[J]. *J Headache Pain*, 2014, 15(1): 72.

[17] Kalita J, Misra UK, Bansal R. Phonophobia and brainstem excitability in migraine[J]. *Eur J Neurosci*, 2021, 53(6): 1988–1997.

[18] Li H, Xu X, Xu R, et al. Latent class analysis of migraine associated vestibular-auditory symptoms[J]. *Cephalalgia*, 2024, 44(6): 3331024241262488. **(Check online resources, the page number information for this document could not be found, please confirm)**

[19] Gopalakrishnan R, Malan NS, Mandava N, et al. Magnetoencephalography studies in migraine and headache disorders: A systematic review[J]. *Headache*, 2025, 65(2): 353–366.

[20] Hsiao FJ, Chen W, Pan LLH, et al. Resting-state magnetoencephalographic oscillatory connectivity to identify patients with chronic migraine using machine learning[J]. *J Headache Pain*, 2022, 23(1): 130.

[21] Leiken K, Xiang J, Zhang F, et al. Magnetoencephalography detection of high-frequency oscillations in the developing brain[J]. *Front Hum Neurosci*, 2014, 8: 969.

[22] Masson R, Lévêque Y, Demarquay G, et al. Auditory attention alterations in migraine: A behavioral and MEG/EEG study[J]. *Clin Neurophysiol*, 2020, 131(8): 1933–1946.

[23] Korostenskaja M, Pardos M, Kujala T, et al. Impaired auditory information processing during acute migraine: A magnetoencephalography study[J]. *Int J Neurosci*, 2011, 121(7): 355–365.

[24] Hipp JF, Hawellek DJ, Corbetta M, et al. Large-scale cortical correlation structure of spontaneous oscillatory activity[J]. *Nat Neurosci*, 2012, 15(6): 884–890.

[25] Zhang X, Wu L, Jia L, et al. MEG analysis of cortical activity and network topology during the interictal period of migraine without aura[J]. *J Integr Neurosci*, 2025, 24(9): 42726.

[26] O'Neill GC, Barratt EL, Hunt BAE, et al. Measuring electrophysiological connectivity by power envelope correlation: A technical review on MEG methods[J]. *Phys Med Biol*, 2015, 60(21): R271–R295.

[27] Wang X, Xiang J, Wang Y, et al. Identification of abnormal neuromagnetic signatures in the motor cortex of adolescent migraine[J]. *Headache*, 2010, 50(6): 1005–1016.

[28] Xiang J, deGrauw X, Korostenskaja M, et al. Altered cortical activation in adolescents with acute migraine: A magnetoencephalography study[J]. *J Pain*, 2013, 14(12): 1553–1563.

[29] Hershey AD. Current approaches to the diagnosis and management of paediatric migraine[J]. *Lancet Neurol*, 2010, 9(2): 190–204.

[30] Tadel F, Baillet S, Mosher JC, et al. Brainstorm: A user-friendly application for MEG/EEG analysis[J]. *Comput Intell Neurosci*, 2011, 2011: 879716.

[31] Colclough GL, Brookes MJ, Smith SM, et al. A symmetric multivariate leakage correction for MEG connectomes[J]. *Neuroimage*, 2015, 117: 439–448.

[32] Maris E, Oostenveld R. Nonparametric statistical testing of EEG- and MEG-data[J]. *J Neurosci Methods*, 2007, 164(1): 177–190.

[33] He P, Li C, Sun W, et al. Differential resting-state MEG microstate patterns in migraineurs: A cross-sectional study[J]. *J Headache Pain*, 2025, 26(1): 215.

[34] Wu D, Zhou Z, Wang Y, et al. Altered neuromagnetic activity under visual stimuli in migraine: A multi-frequency magnetoencephalography study[J]. *Front Neurol*, 2025, 16: 1567150.

[35] Nie W, Zeng W, Yang J, et al. Classification of migraine using static functional connectivity strength and dynamic functional connectome patterns: A resting-state fMRI study[J]. *Brain Sci*, 2023, 13(4): 596.

[36] Chen W, Lin Y, Fuh JL, et al. Sustained visual cortex hyperexcitability in migraine with persistent visual aura[J]. *Brain*, 2011, 134(8): 2387–2395.

[37] Bassez I, Van de Steen F, Hackl S, et al. Investigation on how dynamic effective connectivity patterns encode the fluctuating pain intensity in chronic migraine[J]. *Neurobiol Pain*, 2022, 12: 100100.

[38] Cocores AN, Smirnoff L, Greco G, et al. Update on neuromodulation for migraine and other primary headache disorders: Recent advances and new indications[J]. *Curr Pain Headache Rep*, 2025, 29(1): 47.